

# Using a diphenyl-bi-(1,2,4-triazole) tricarbonylrhenium(I) complex with intramolecular $\pi$ - $\pi$ stacking interaction for efficient solid-state luminescence enhancement

Alexandre Poirot, Corinne Vanucci-Bacqu , B atrice Delavaux-Nicot, Clarisse Meslien, Nathalie Saffon-Merceron, Charles-Louis Serpentini, Florence Bedos-Belval, Eric Benoist and Suzanne Fery-Forgues

## Synthesis and characterization

<b>Figure S1.</b> Carbon numbering for attribution of $^1\text{H}$ and $^{13}\text{C}$ NMR chemical shifts .....	2
<b>Figure S2.</b> $^1\text{H}$ NMR spectrum of complex <b>Re-BPTA</b> in $\text{CDCl}_3$ .....	2
<b>Figure S3.</b> $^{13}\text{C}$ NMR spectrum of complex <b>Re-BPTA</b> in $\text{CDCl}_3$ .....	3
<b>Figure S4.</b> NMR HSQC spectrum of complex <b>Re-BPTA</b> in $\text{CDCl}_3$ .....	3
<b>Figure S5.</b> Experimental and theoretical mass spectra of <b>Re-BPTA</b> .....	4
<b>Figure S6.</b> Variable temperature $^1\text{H}$ NMR spectra of complex <b>Re-BPTA</b> in $\text{C}_2\text{D}_2\text{Cl}_4$ at 400 MHz .....	5

## Crystallographic data

<b>Table S1.</b> Selected bond lengths ( $\text{Å}$ ) and angles ( $^\circ$ ) for ligand <b>BPTA</b> .....	5
<b>Table S2.</b> Selected bond lengths ( $\text{Å}$ ) and angles ( $^\circ$ ) for complex <b>Re-BPTA</b> .....	6
<b>Figure S7.</b> Crystallographic arrangement of ligand <b>BPTA</b> .....	7
<b>Figure S8.</b> Crystallographic arrangement of complex <b>Re-BPTA</b> .....	7

## Quantum chemistry calculations

<b>Figure S9.</b> Structure of <b>Re-BPTA</b> in the ground and lowest excited triplet state calculated by DFT .....	8
<b>Table S3.</b> Composition (%) of the frontier molecular orbitals of complex <b>Re-BPTA</b> in $\text{CH}_2\text{Cl}_2$ .....	8
<b>Table S4.</b> Main electronic transitions for complex <b>Re-BPTA</b> in $\text{CH}_2\text{Cl}_2$ calculated using TD-DFT .....	9
<b>Figure S10.</b> Main electronic transitions, theoretical and experimental UV-vis absorption spectra of <b>Re-BPTA</b> in $\text{CH}_2\text{Cl}_2$ .....	9
<b>Figure S11.</b> Representation of complex <b>Re-BPTA</b> in the lowest triplet excited state. Spin density. Position of unpaired electrons in the hole (HOMO) and in the particle (LUMO) .....	9
<b>Table S5.</b> Selected bond lengths ( $\text{Å}$ ), distance between the centroids (Cd) of both phenyl rings, and angles ( $^\circ$ ) for complex <b>Re-BPTA</b> in the ground state and in the lowest triplet excited state ( $^3\text{MLCT}$ ) calculated by DFT .....	10

## Electrochemistry

<b>Table S6.</b> Selected electrochemical data of complex <b>Re-BPTA</b> . Comparison with <b>Re-Phe</b> and <b>Re-PBO</b> .....	11
<b>Table S7.</b> Experimental electrochemical data and calculated value of the electrochemical energy gap ( $E_g^{\text{el}}$ ) .....	11
<b>Evaluation of the energy gap values (<math>E_g^{\text{el}}</math>) for the Re complexes</b> .....	11
<b>Figure S12.</b> OSWVs: anodic and cathodic scans of complex <b>Re-BPTA</b> .....	12
<b>Figure S13.</b> Cyclic voltammograms of complex <b>Re-BPTA</b> at 0.2 V/s, and segmented voltammogram at 1 V/s ....	12
<b>Figure S14.</b> Segmented cyclic voltammograms of <b>Re-BPTA</b> at 10 V/s and at increasing potential .....	12
<b>Figure S15.</b> Cyclic voltammograms of complex <b>Re-BPTA</b> first oxidation wave at 50 V/s and 100 V/s .....	13
<b>Figure S16.</b> OSWVs: anodic and cathodic scans of ligand <b>BPTA</b> .....	13
<b>Figure S17.</b> Cyclic voltammograms of ligand <b>BPTA</b> at 0.2 V/s .....	13

## Spectroscopy

<b>Table S8.</b> Solid state spectroscopic data of two samples of <b>Re-BPTA</b> crystallized in butanol and $\text{CHCl}_3$ .....	14
<b>Figure S18.</b> Emission spectra of complex <b>Re-BPTA</b> in acetonitrile solutions containing from 0 to 95% water, 24h after sample preparation. Evolution of the PL intensity at 546 nm as a function of $f_w$ .....	14
<b>Figure S19.</b> Normalized emission spectra of microcrystals of <b>Re-BPTA</b> obtained from butanol as powder and after dispersion in water, and comparison with the suspension in $\text{H}_2\text{O}/\text{CH}_3\text{CN}$ 90:10 v/v (AIPE experiment) ..	14
<b>Figure S20.</b> Photoluminescence decay of <b>Re-BPTA</b> in dichloromethane solution .....	15
<b>Figure S21.</b> Photoluminescence decay of <b>Re-BPTA</b> in acetonitrile solution .....	15
<b>Figure S22.</b> Photoluminescence decay of <b>Re-BPTA</b> in methanol solution .....	16
<b>Figure S23.</b> Photoluminescence decay of <b>Re-BPTA</b> microcrystalline powder .....	16
<b>Figure S24.</b> Photoluminescence decay of <b>Re-BPTA</b> in water/acetonitrile 90:10 v/v .....	17
<b>Figure S25.</b> Photoluminescence decay of <b>Re-BPTA</b> as microcrystalline powder dispersed in water .....	17
<b>Figure S26.</b> Photoluminescence decay of <b>Re-Phe</b> microcrystalline powder .....	18
<b>Figure S27.</b> Photoluminescence decay of <b>Re-Phe-Ada</b> microcrystalline powder .....	18

## Synthesis and characterization

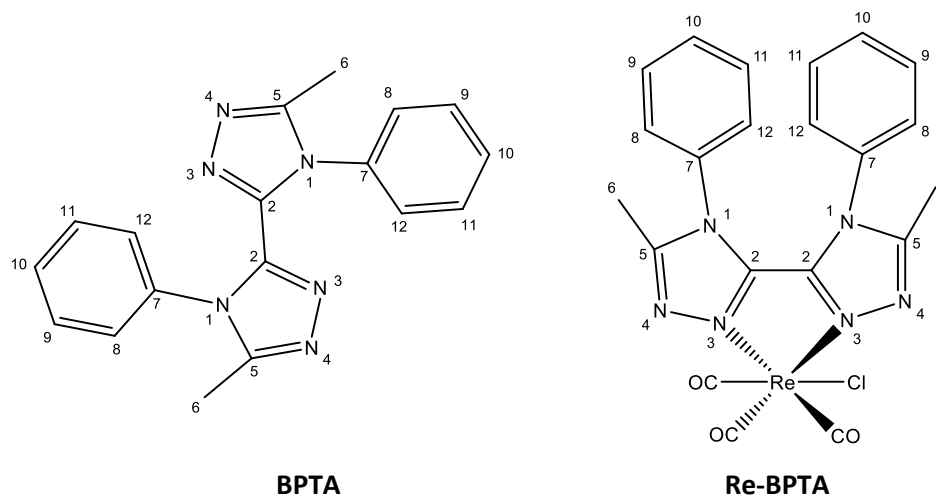


**Figure S1.** Carbon numbering for attribution of  $^1\text{H}$  and  $^{13}\text{C}$  NMR chemical shifts.

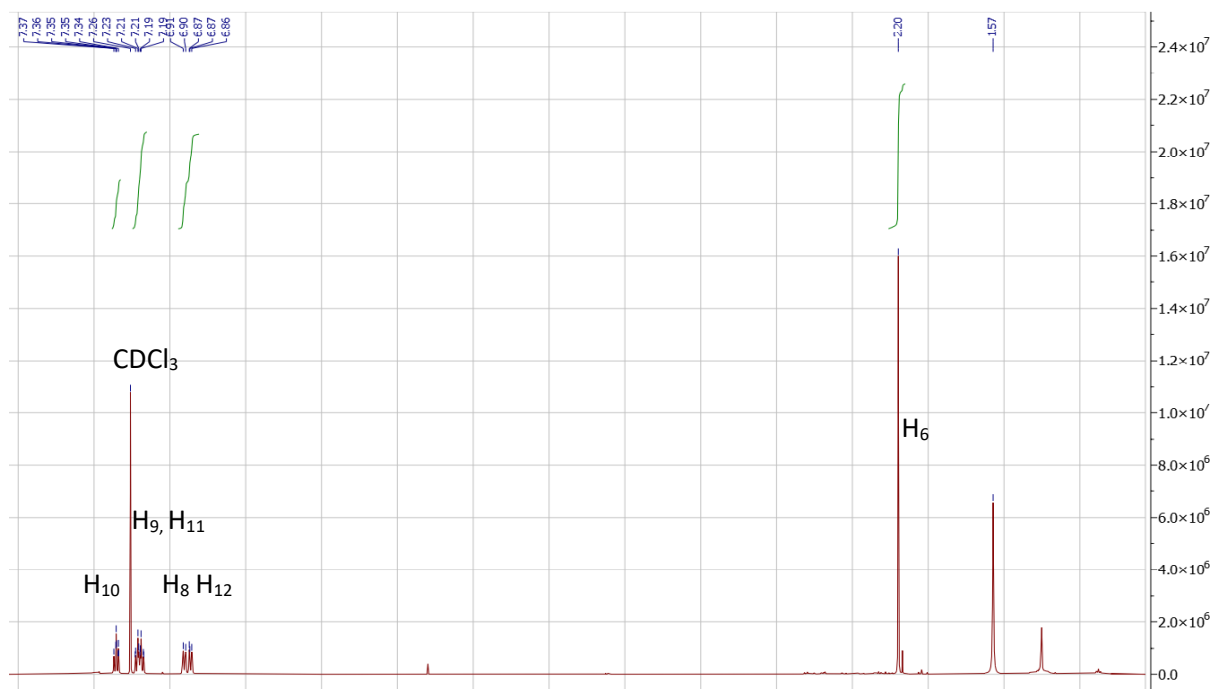


**Figure S2.**  $^1\text{H}$  NMR spectrum (500 MHz) of complex **Re-BPTA** in  $\text{CDCl}_3$  recorded at  $25^\circ\text{C}$ .

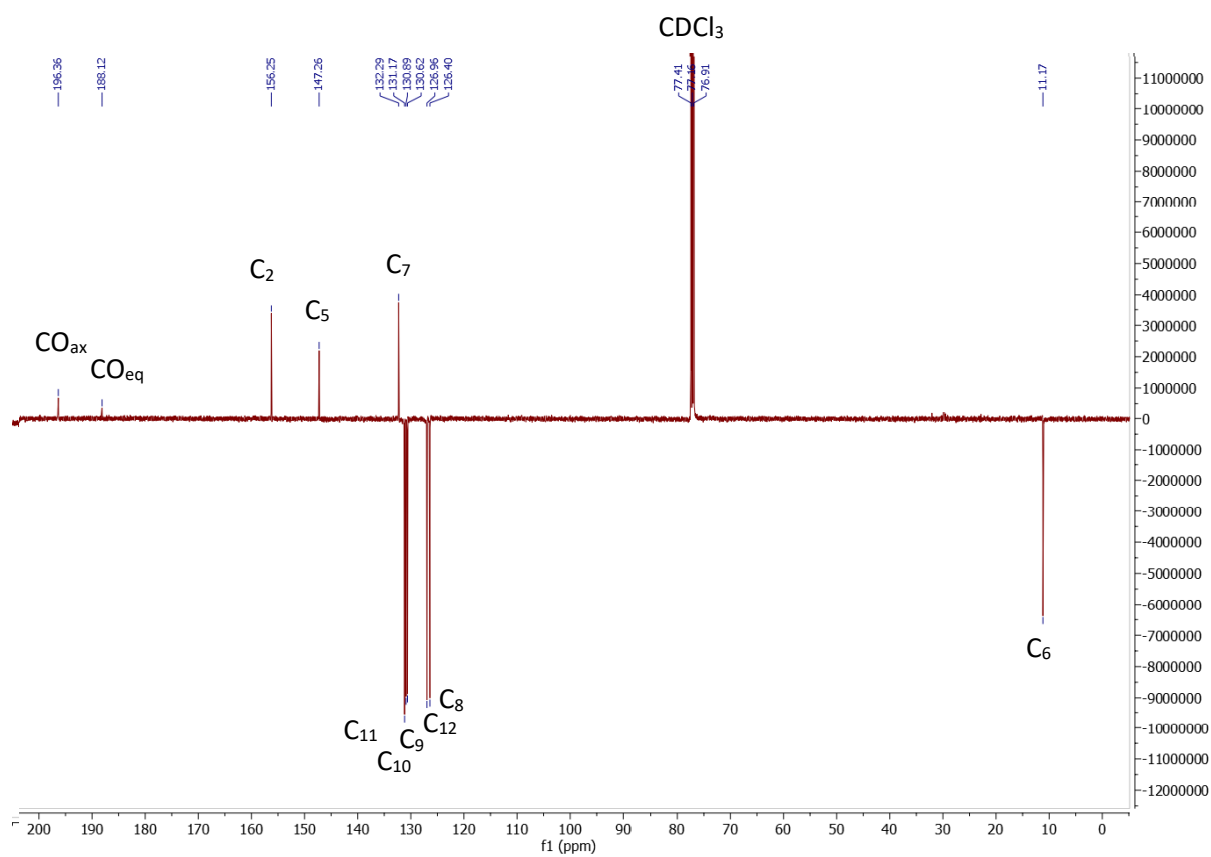


**Figure S3.**  $^{13}\text{C}$  NMR spectrum (125 MHz, JMod) of complex **Re-BPTA** in  $\text{CDCl}_3$  recorded at  $25^\circ\text{C}$ .

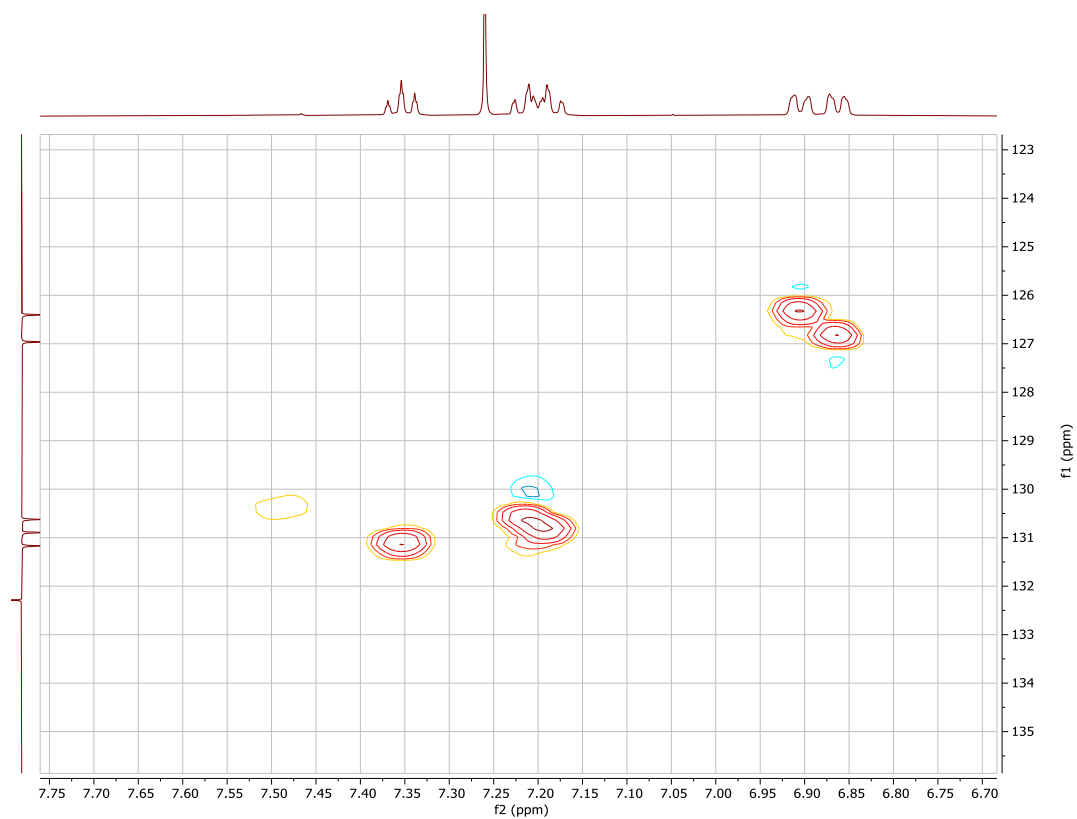


**Figure S4.** HSQC NMR spectrum of complex **Re-BPTA** in  $\text{CDCl}_3$ .

Cone voltage = 30 V XEVO G2 QTOF 04-Jun-2021 09:32:36  
Re-BPTA i 82 (0.509) AM2 (Ar,20000.0,0.00,0.00); Cm (79:87-45:55x2.000) 1: TOF MS ES+  
3.79e5

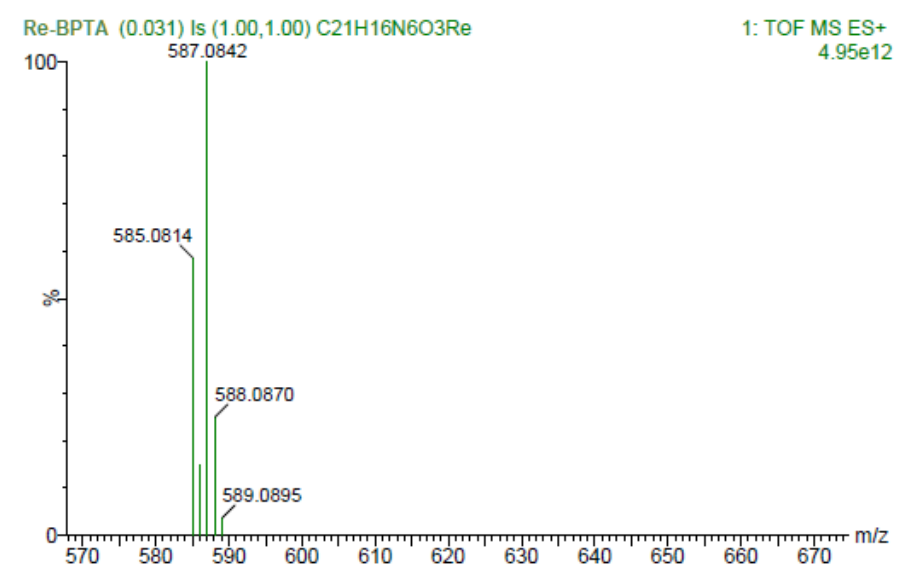
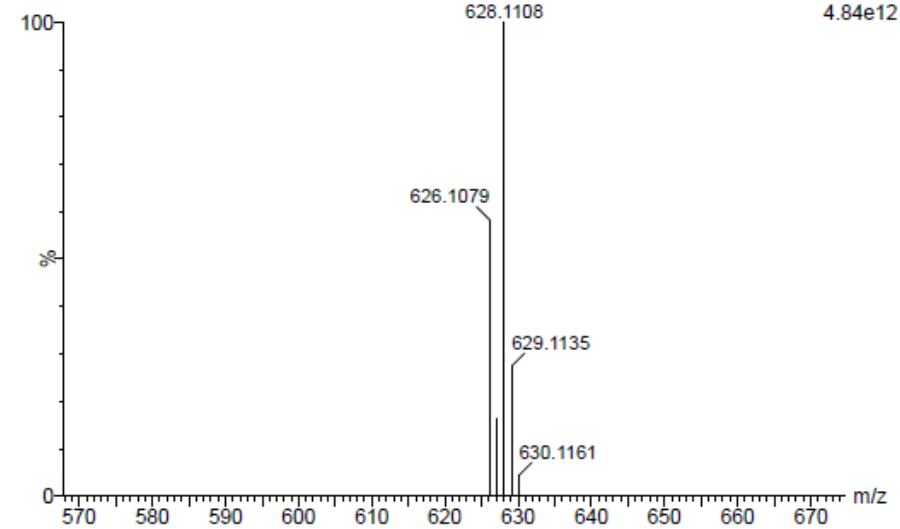
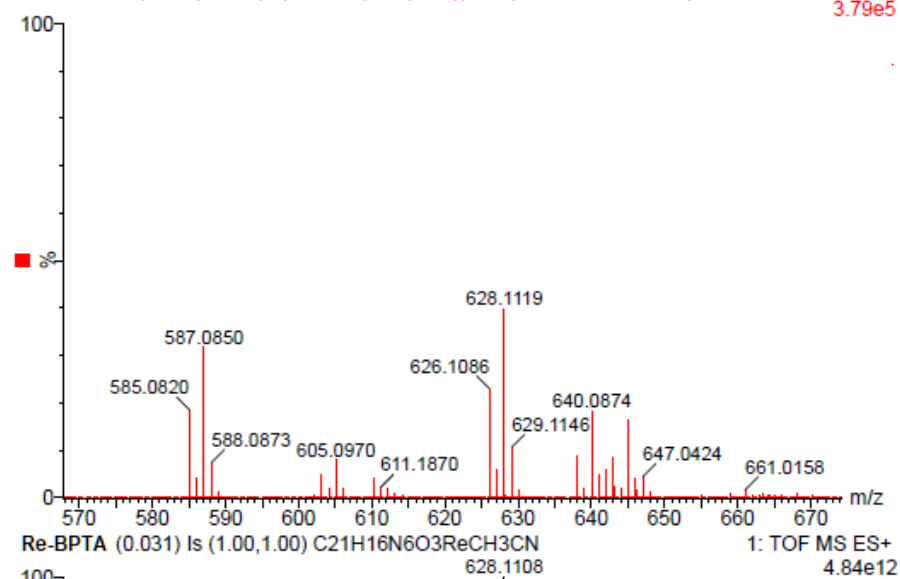
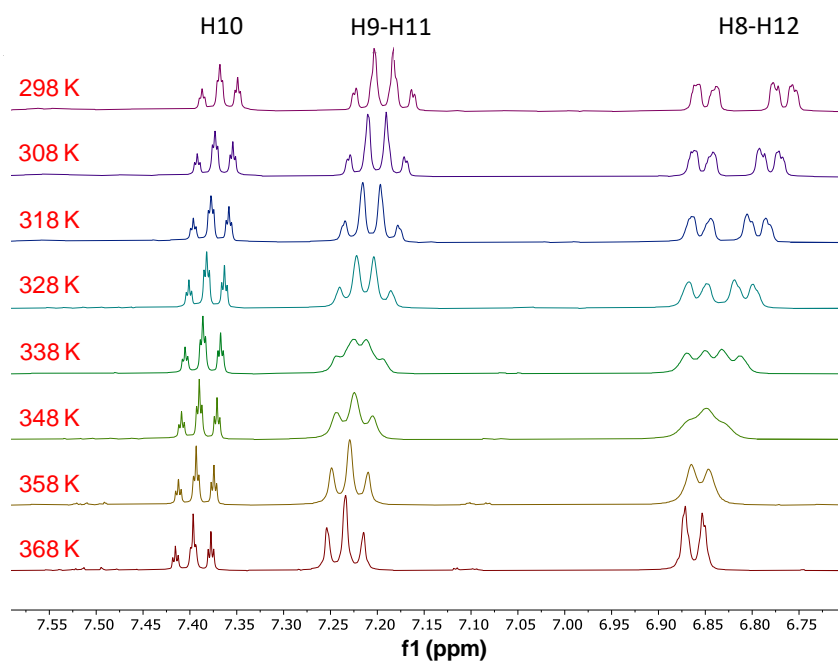


Figure S5. Experimental (top) and theoretical (middle and bottom) mass spectra of **Re-BPTA**.

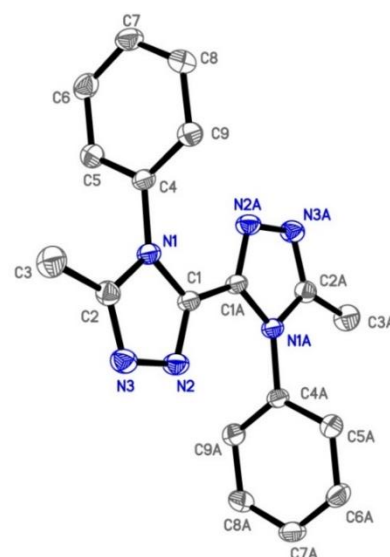


**Figure S6.** Variable temperature  $^1\text{H}$ NMR spectra of complex **Re-BPTA** in  $\text{C}_2\text{D}_2\text{Cl}_4$  at 400 MHz.

### Crystallographic data

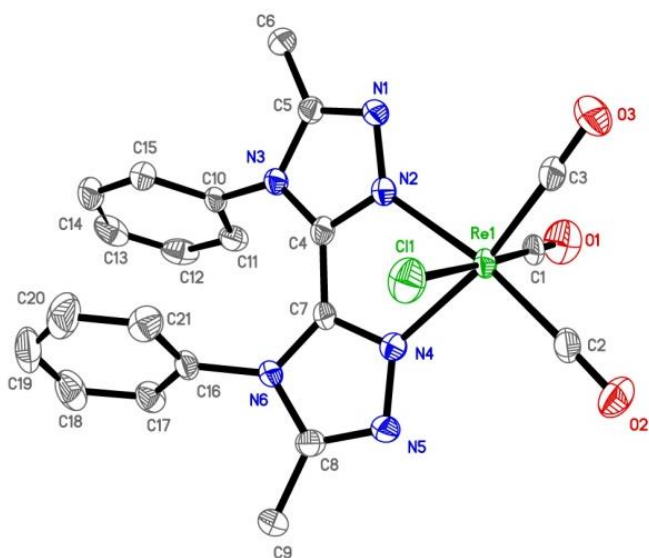
**Table S1.** Selected bond lengths ( $\text{\AA}$ ) and angles ( $^\circ$ ) for ligand **BPTA**. The atoms are numbered like on the molecular view.

Bond	D ( $\text{\AA}$ )	Bond angle	Angle value ( $^\circ$ )
N(1)-C(2)	1.3700(12)	C(2)-N(1)-C(1)	104.49(8)
N(1)-C(1)	1.3741(11)	C(2)-N(1)-C(4)	124.61(8)
N(1)-C(4)	1.4438(11)	C(1)-N(1)-C(4)	130.86(8)
N(2)-C(1)	1.3151(11)	C(1)-N(2)-N(3)	107.21(8)
N(2)-N(3)	1.3876(12)	C(2)-N(3)-N(2)	107.40(8)
N(3)-C(2)	1.3133(12)	N(2)-C(1)-N(1)	110.39(8)
C(1)-C(1A)	1.4574(18)	N(2)-C(1)-C(1A)	124.90(10)
C(2)-C(3)	1.4835(14)	N(1)-C(1)-C(1A)	124.71(10)
C(4)-C(9)	1.3859(13)	N(3)-C(2)-N(1)	110.50(8)
C(4)-C(5)	1.3881(13)	N(3)-C(2)-C(3)	125.77(9)
C(5)-C(6)	1.3910(14)	N(1)-C(2)-C(3)	123.71(9)
C(6)-C(7)	1.3833(16)	C(9)-C(4)-C(5)	121.97(9)
C(7)-C(8)	1.3878(16)	C(9)-C(4)-N(1)	119.56(8)
C(8)-C(9)	1.3940(14)	C(5)-C(4)-N(1)	118.40(8)
		C(4)-C(5)-C(6)	118.63(9)
		C(7)-C(6)-C(5)	120.25(9)
		C(6)-C(7)-C(8)	120.46(9)
		C(7)-C(8)-C(9)	120.14(10)
		C(4)-C(9)-C(8)	118.55(9)



**Table S2.** Selected bond lengths (Å) and angles (°) for complex **Re-BPTA**. The atoms are numbered like on the molecular view.

Bond	D (Å)	Bond angle	Angle value (°)
Re(1)-C(3)	1.908(4)	C(3)-Re(1)-C(2)	91.59(17)
Re(1)-C(2)	1.925(4)	C(3)-Re(1)-C(1)	89.97(18)
Re(1)-C(1)	1.960(5)	C(2)-Re(1)-C(1)	91.71(18)
Re(1)-N(2)	2.175(3)	C(3)-Re(1)-N(2)	97.45(15)
Re(1)-N(4)	2.179(3)	C(2)-Re(1)-N(2)	170.70(15)
Re(1)-Cl(1)	2.4553(11)	C(1)-Re(1)-N(2)	90.50(15)
O(1)-C(1)	1.091(5)	C(3)-Re(1)-N(4)	168.98(15)
O(2)-C(2)	1.141(5)	C(2)-Re(1)-N(4)	97.19(15)
O(3)-C(3)	1.154(5)	C(1)-Re(1)-N(4)	96.40(15)
N(1)-C(5)	1.312(5)	N(2)-Re(1)-N(4)	73.59(12)
N(1)-N(2)	1.383(4)	C(3)-Re(1)-Cl(1)	91.80(14)
N(2)-C(4)	1.318(5)	C(2)-Re(1)-Cl(1)	91.36(13)
N(3)-C(4)	1.357(5)	C(1)-Re(1)-Cl(1)	176.41(13)
N(3)-C(5)	1.383(5)	N(2)-Re(1)-Cl(1)	86.17(10)
N(3)-C(10)	1.446(5)	N(4)-Re(1)-Cl(1)	81.37(10)
N(4)-C(7)	1.312(5)	C(5)-N(1)-N(2)	106.2(3)
N(4)-N(5)	1.378(4)	C(4)-N(2)-N(1)	108.6(3)
N(5)-C(8)	1.318(5)	C(4)-N(2)-Re(1)	116.8(3)
N(6)-C(7)	1.363(5)	N(1)-N(2)-Re(1)	133.5(2)
N(6)-C(8)	1.373(5)	C(4)-N(3)-C(5)	104.6(3)
N(6)-C(16)	1.448(5)	C(4)-N(3)-C(10)	129.0(3)
C(4)-C(7)	1.446(5)	C(5)-N(3)-C(10)	125.3(3)
		C(7)-N(4)-N(5)	109.1(3)
		C(7)-N(4)-Re(1)	116.2(3)
		N(5)-N(4)-Re(1)	131.9(3)
		C(8)-N(5)-N(4)	105.9(3)
		C(7)-N(6)-C(8)	104.8(3)
		C(7)-N(6)-C(16)	127.2(3)
		C(8)-N(6)-C(16)	125.8(3)



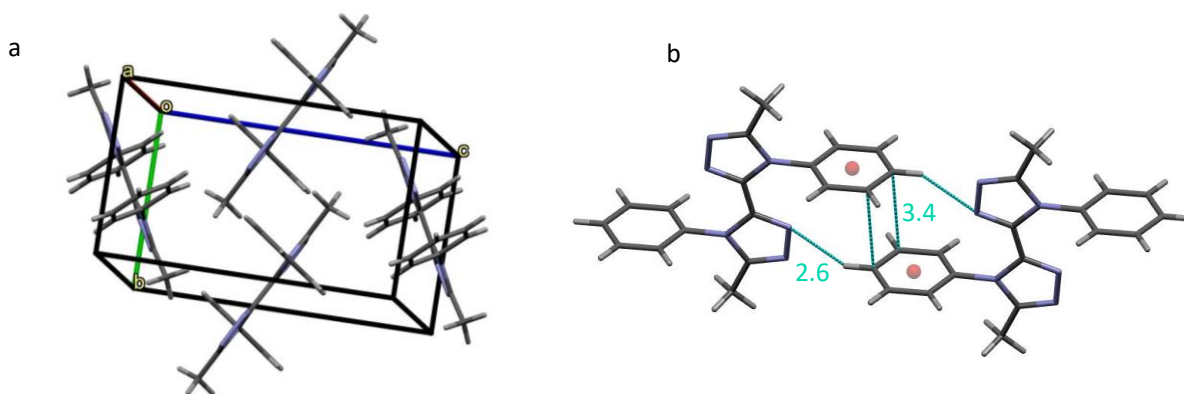


**Figure S7.** Crystallographic arrangement of ligand **BPTA**: a) asymmetric unit. b) Short contacts (drawn in turquoise ink) between neighboring molecules. The centroid-to-centroid distance between the phenyl rings is  $\sim 4.1$  Å. All distances are in Å.

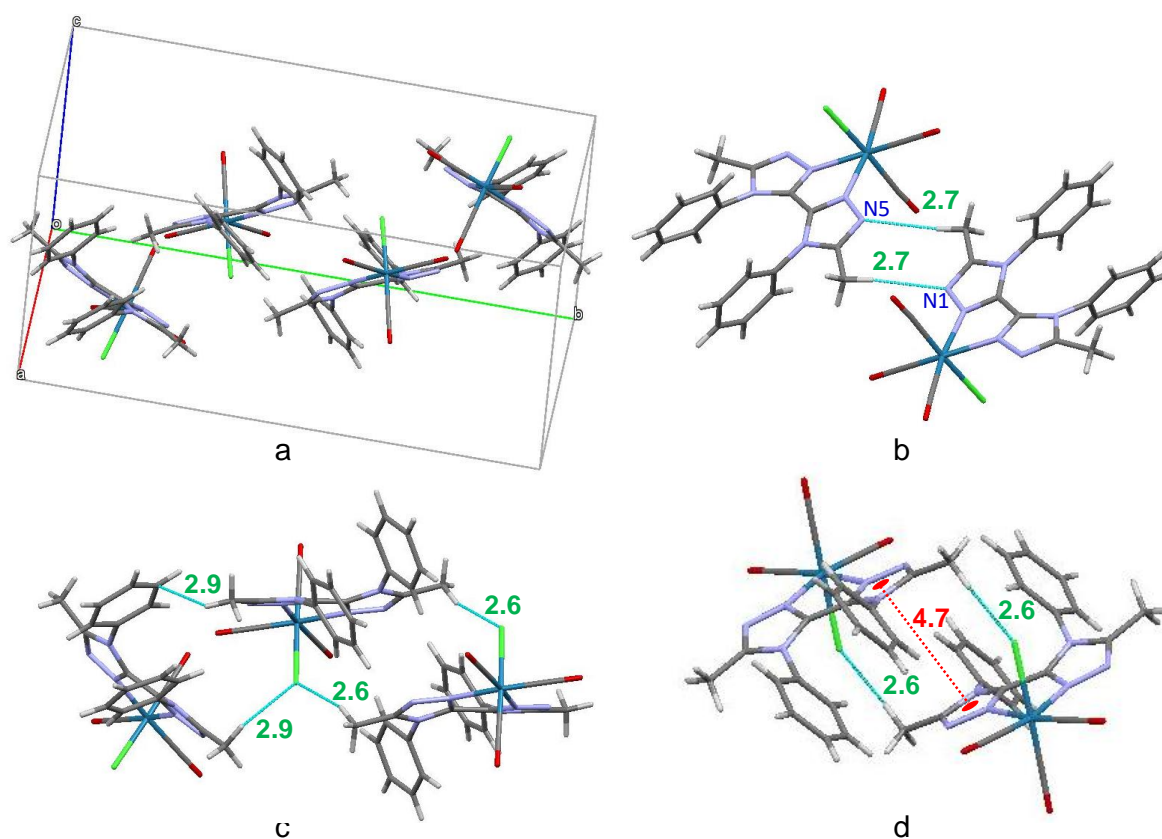


**Figure S8.** Crystallographic arrangement of complex **Re-BPTA**: a) asymmetric unit. b) Short contacts (drawn in turquoise ink) involving the nitrogen atoms. c) Short contacts (drawn in turquoise ink) involving the halogen atoms and one C...H interaction and d) centroid-to-centroid distance (in red ink) between triazole rings. All distances are in Å.

## Quantum chemistry calculations

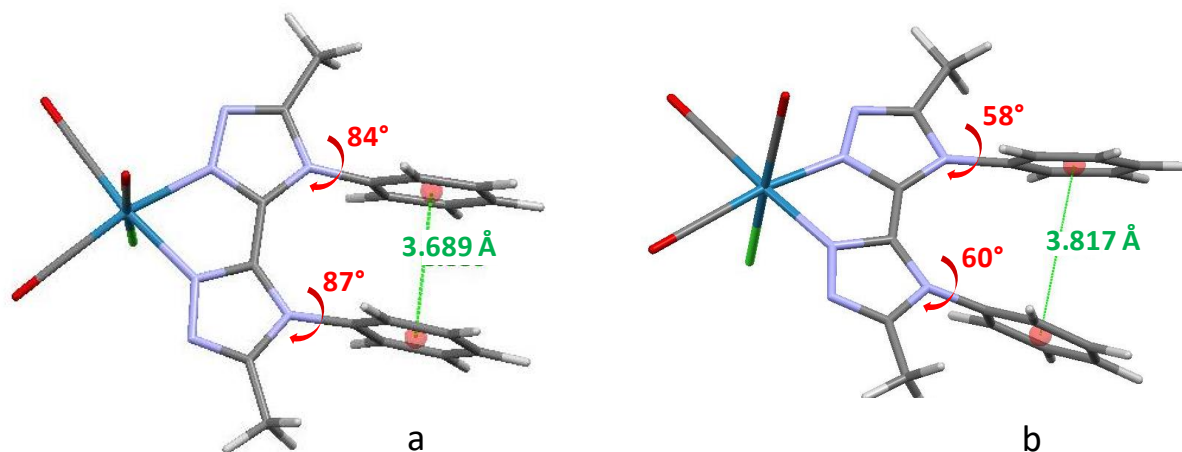


**Figure S9.** Structure of **Re-BPTA** in the ground state (a) and in the lowest excited triplet state (b) calculated by DFT at the PBE0/LANL2DZ level of theory. Angles between the planes of the phenyl and triazole rings are indicated in red ink. The distance between centroids is indicated in green ink.

**Table S3.** Composition (%) of the frontier molecular orbitals involved in the main electronic transitions of complex **Re-BPTA** in  $\text{CH}_2\text{Cl}_2$ , calculated using the TD-DFT method at the PBE0/LANL2DZ level,

	Rhenium	Cl	Phenyl	Triazole	CO
HOMO-9	8.516	14.778	48.574	24.608	3.524
HOMO-8	8.913	17.895	41.667	27.879	3.646
HOMO-6	14.088	61.658	5.889	12.705	5.660
HOMO-5	0.003	0.019	99.693	0.283	0.001
HOMO-4	0.470	5.242	80.648	13.449	0.190
HOMO-3	2.515	35.304	9.102	51.659	1.419
HOMO-2	68.403	0.636	0.079	1.591	29.291
HOMO-1	46.753	27.047	0.351	5.249	20.599
HOMO	47.371	22.356	0.0541	6.985	23.233
LUMO	3.711	2.267	2.450	84.096	7.477
LUMO+1	0.306	0.050	93.877	5.100	0.667
LUMO+2	17.789	0.715	6.017	-0.216	75.696
LUMO+3	7.533	1.175	65.937	1.219	24.135
LUMO+4	10.461	1.744	34.944	14.157	38.694
LUMO+5	2.045	0.176	83.911	5.348	8.520



**Table S4.** Description of the main electronic transitions for complex **Re-BPTA** in  $\text{CH}_2\text{Cl}_2$  calculated using the TD-DFT method at the PBE0/LANL2DZ level, with corresponding wavelength ( $\lambda$ ), energy ( $E$ ) and oscillator strength ( $f$ ). Only orbitals contributing by more than 5% have been indicated, and they are listed in decreasing order of importance. phe: phenyl; ta: *bi*-triazole.

Electronic transition	Contribution	Assignment		$\lambda$ (nm)	$E$ (eV)	$f$
S0 $\rightarrow$ S2	H-1 $\rightarrow$ LUMO	$d(\text{Re}) + p(\text{Cl}) + \pi(\text{CO}) \rightarrow \pi^*(\text{ta}) + \pi^*(\text{CO})$	MLCT/XLCT/LLCT	392.7	3.16	0.134
S0 $\rightarrow$ S7	H-4 $\rightarrow$ LUMO	$\pi(\text{phe}) + \pi(\text{ta}) + p(\text{Cl}) \rightarrow \pi^*(\text{ta}) + \pi^*(\text{CO})$	IL/LLCT	294	4.22	0.036
S0 $\rightarrow$ S10	H-6 $\rightarrow$ LUMO	$p(\text{Cl}) + d(\text{Re}) + \pi(\text{ta}) + \pi(\text{phe}) + \pi(\text{CO}) \rightarrow \pi^*(\text{ta}) + \pi^*(\text{CO})$	XLCT/MLCT	290.6	4.27	0.117
S0 $\rightarrow$ S14	H-1 $\rightarrow$ LUMO+1	$d(\text{Re}) + p(\text{Cl}) + \pi(\text{CO}) \rightarrow \pi^*(\text{phe}) + \pi^*(\text{ta})$	MLCT/LLCT	268.3	4.62	0.045
S0 $\rightarrow$ S17	H-8 $\rightarrow$ LUMO	$\pi(\text{phe}) + \pi(\text{ta}) + p(\text{Cl}) + d(\text{Re}) \rightarrow \pi^*(\text{ta}) + \pi^*(\text{CO})$	IL/LLCT/XLCT/MLCT	262.7	4.72	0.041
S0 $\rightarrow$ S22	H-9 $\rightarrow$ LUMO	$\pi(\text{phe}) + \pi(\text{ta}) + p(\text{Cl}) + d(\text{Re}) \rightarrow \pi^*(\text{ta}) + \pi^*(\text{CO})$	IL/LLCT/XLCT/MLCT	249.8	4.96	0.128
S0 $\rightarrow$ S51	H-6 $\rightarrow$ LUMO+4	$p(\text{Cl}) + d(\text{Re}) + \pi(\text{ta}) + \pi(\text{phe}) + \pi(\text{CO}) \rightarrow \pi^*(\text{CO}) + \pi^*(\text{phe}) + \pi^*(\text{ta}) + p(\text{Re})$	XLCT	213.2	5.82	0.042

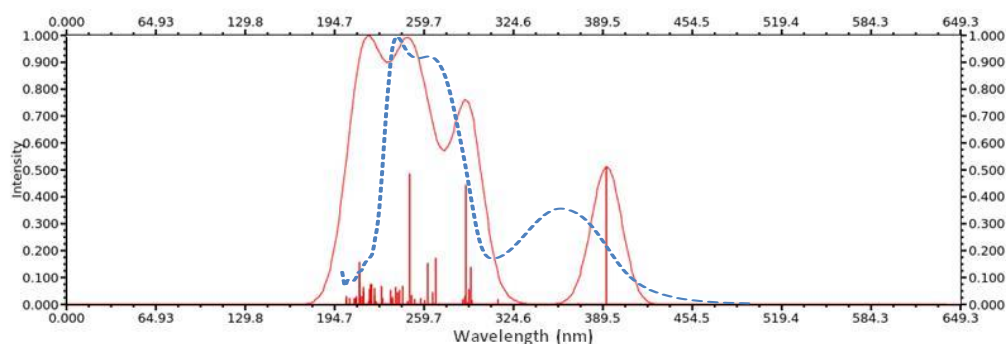


**Figure S10.** Main electronic transitions calculated using the TD-DFT method at the PBE0/LANL2DZ level and theoretical UV-vis absorption spectrum (red lines), compared with the experimental spectrum (blue line), for complex **Re-BPTA** in  $\text{CH}_2\text{Cl}_2$ .

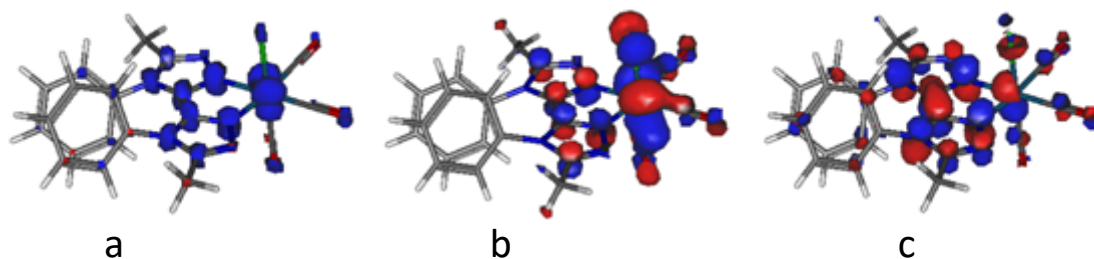
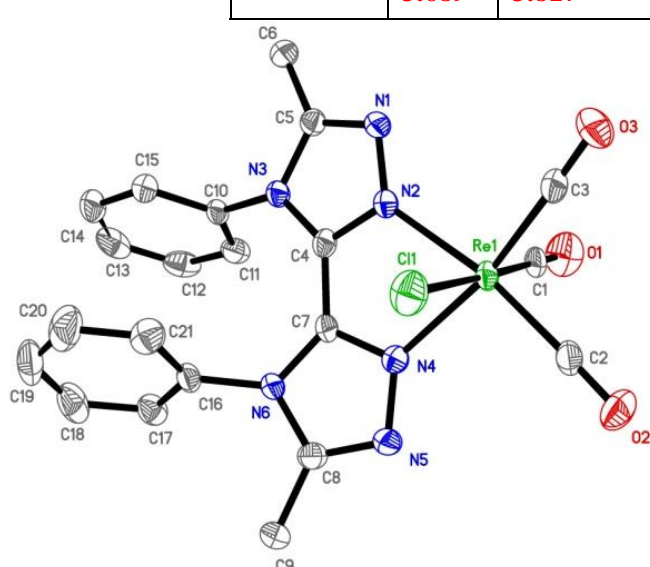


**Figure S11.** Representation of complex **Re-BPTA** in the lowest triplet excited state ( $^3\text{MLCT}$ ) calculated by DFT at the PBE0/LANL2DZ level of theory. a) Spin density distribution (isovalue =  $0.03 \text{ e bohr}^{-3}$ ). b) Position of unpaired electrons in the hole (HOMO) and (c) in the particle (LUMO). Data obtained from the comparison of the Kohn-Sham orbitals of the molecule in the triplet state with those of the ground state.

**Table S5.** Selected bond lengths (Å), distance between the centroids (Cd) of both phenyl rings, and angles (°) for complex **Re-BPTA** in the ground state and in the lowest triplet excited state (<sup>3</sup>MLCT) calculated by DFT at the PBE0/LANL2DZ level of theory. The atoms are numbered like on the molecular view.

Bond	D (Å)		Bond angle	Angle value (°)	
	Ground state	Lowest triplet excited state		Ground state	Lowest triplet excited state
Re(1)-C(3)	1.910	1.944	C(3)-Re(1)-C(2)	91.08	88.56
Re(1)-C(2)	1.909	1.943	C(3)-Re(1)-C(1)	90.81	91.99
Re(1)-C(1)	1.887	1.925	C(2)-Re(1)-C(1)	90.82	91.95
Re(1)-N(2)	2.129	2.063	C(3)-Re(1)-N(2)	97.04	97.50
Re(1)-N(4)	2.128	2.058	C(2)-Re(1)-N(2)	169.45	172.84
Re(1)-Cl(1)	2.544	2.514	C(1)-Re(1)-N(2)	95.00	91.66
O(1)-C(1)	1.191	1.178	C(3)-Re(1)-N(4)	169.82	172.72
O(2)-C(2)	1.184	1.177	C(2)-Re(1)-N(4)	97.27	97.35
O(3)-C(3)	1.184	1.177	C(1)-Re(1)-N(4)	93.88	92.05
N(1)-C(5)	1.336	1.330	N(2)-Re(1)-N(4)	73.57	76.33
N(1)-N(2)	1.380	1.386	C(3)-Re(1)-Cl(1)	91.17	88.64
N(2)-C(4)	1.347	1.410	C(2)-Re(1)-Cl(1)	91.02	89.07
N(3)-C(4)	1.371	1.393	C(1)-Re(1)-Cl(1)	177.25	178.81
N(3)-C(5)	1.393	1.406	N(2)-Re(1)-Cl(1)	82.87	87.27
N(3)-C(10)	1.443	1.435	N(4)-Re(1)-Cl(1)	83.86	87.21
N(4)-C(7)	1.346	1.411	C(5)-N(1)-N(2)	106.22	107.04
N(4)-N(5)	1.380	1.386	C(4)-N(2)-N(1)	109.74	109.00
N(5)-C(8)	1.337	1.330	C(4)-N(2)-Re(1)	118.60	117.33
N(6)-C(7)	1.371	1.392	N(1)-N(2)-Re(1)	131.06	133.66
N(6)-C(8)	1.392	1.406	C(4)-N(3)-C(5)	106.04	106.03
N(6)-C(16)	1.443	1.435	C(4)-N(3)-C(10)	131.16	127.22
C(4)-C(7)	1.441	1.381	C(5)-N(3)-C(10)	122.67	124.66
<b>Cd-Cd</b>	<b>3.689</b>	<b>3.817</b>	C(7)-N(4)-N(5)	109.73	109.00
			C(7)-N(4)-Re(1)	118.84	117.35
			N(5)-N(4)-Re(1)	131.42	133.47
			C(8)-N(5)-N(4)	106.20	107.02
			C(7)-N(6)-C(8)	106.03	106.04
			C(7)-N(6)-C(16)	131.13	127.38
			C(8)-N(6)-C(16)	122.75	124.46



## Electrochemistry

**Table S6.** Selected electrochemical data of complex **Re-BPTA** [ $1.0 \times 10^{-3}$  M]. Values determined by OSWV on a Pt working electrode in  $\text{CH}_2\text{Cl}_2 + 0.1$  M  $n\text{-Bu}_4\text{NBF}_4$  at room temperature.<sup>a,b</sup> Ferrocene was used as internal reference. Comparison with **Re-Phe** and **Re-PBO**.

Compound	Oxidation		Reduction		
	$E_2$	$E_1$	$E_1$	$E_2$	$E_3$
<b>Re-BPTA</b>	1.66	1.37	-1.51	-1.66 <sup>e</sup>	
<b>Re-Phe</b> <sup>f</sup>	1.78	1.46	-1.29 <sup>c</sup>	-1.78	
<b>Re-PBO</b> <sup>g</sup>	1.73	1.44	-1.28 <sup>d</sup>	-1.58	-1.83

<sup>a</sup> OSWVs were obtained using a sweep width of 20 mV, a frequency of 20 Hz, and a step potential of 5 mV.

<sup>b</sup> Potential values in Volts vs. SCE ( $\text{Fc}^+/\text{Fc}$  is observed at  $0.55 \text{ V} \pm 0.01 \text{ V vs. SCE}$ ).

<sup>c</sup> One-electron quasi-reversible process at 1 V/s.

<sup>d</sup> One-electron quasi-reversible process at 0.2 V/s

<sup>e</sup> Shoulder of weak intensity.

<sup>f</sup> Values from Poirot *et al.*, *Dalton Trans.*, 2021, **50**, 13686-13698 (ESI). DOI: [10.1039/D1DT02161C](https://doi.org/10.1039/D1DT02161C)

<sup>g</sup> Values from Wang *et al.* *Dalton Trans.*, 2019, **48**, 15906–15916 (ESI). DOI: [10.1039/c9dt02786f](https://doi.org/10.1039/c9dt02786f)

**Table S7.** Experimental electrochemical data used, and calculated value of the electrochemical energy gap ( $E_g^{\text{el}}$ ) for mentioned complexes

Compound	$E_{\text{onset ox}}$ (V)	$E_{\text{onset red}}$ (V)	$E_{\text{HOMO}}$ (eV)	$E_{\text{LUMO}}$ (eV)	$E_g^{\text{el}}$ (eV)
<b>Re-BPTA</b>	1.10	-1.60	-5.84	-3.14	2.70
<b>Re-Phe</b> <sup>a</sup>	1.42	-1.23	-6.16	-3.51	2.65

<sup>a</sup> Values from Poirot *et al.*, *Dalton Trans.*, 2021, **50**, 13686-13698 (ESI). DOI: [10.1039/D1DT02161C](https://doi.org/10.1039/D1DT02161C)

### Evaluation of the energy gap values ( $E_g^{\text{el}}$ ) for the Re complexes

The onset oxidation and reduction potentials ( $E_{\text{onset ox}}$ ,  $E_{\text{onset red}}$ ) were measured by cyclic voltammetry in volt *versus* SCE. The CVs were carried out at a potential scan rate of  $200 \text{ mV s}^{-1}$  at room temperature.

The HOMO and LUMO energy levels ( $E_{\text{HOMO}}$  and  $E_{\text{LUMO}}$ ) in electron volt (eV) were calculated according to the empirical equations (1) and (2):<sup>[1]</sup>

$$E_{\text{HOMO}} (\text{eV}) = -e (E_{\text{onset ox}} (\text{V vs. SCE}) + 4.74 \text{ V}) \quad \text{Eq(1)}$$

$$E_{\text{LUMO}} (\text{eV}) = -e (E_{\text{onset red}} (\text{V vs. SCE}) + 4.74 \text{ V}) \quad \text{Eq(2)}$$

and the energy gap value was obtained as follows:  $E_g^{\text{el}} = (E_{\text{LUMO}} - E_{\text{HOMO}})$ .

The differences observed for the estimation of the energy gaps using experimental methods or theoretical calculations are well known. See for example: R. Stowasser and R. Hoffmann, *J. Am. Chem. Soc.* 1999, **121**, 3414-3420.

[1] a) Y. Zhou, J. W. Kim, R. Nandhakumar, M. J. Kim, E. Cho, Y. S. Kim, Y. H. Jang, C. Lee, S. Han, K. M. Kim, J.-J. Kim and J. Yoon, *Chem. Commun.* 2010, **46**, 6512–6514 and references therein; b) G. V. Loukova, *Chem. Phys. Lett.* 2002, **353**, 244–252.

## Electrochemical selected curves

**OSWV study** was performed on a Pt working electrode in  $\text{CH}_2\text{Cl}_2 + 0.1 \text{ M } n[\text{Bu}_4\text{N}][\text{BF}_4]$  at room temperature in the presence of ferrocene used as internal reference. Frequency 20 Hz, amplitude 20 mV, step potential 5 mV.

**Cyclic voltammograms** of compound **Re-BPTA** and ligand **BPTA** were performed on a Pt working electrode in  $\text{CH}_2\text{Cl}_2 + 0.1 \text{ M } n[\text{Bu}_4\text{N}][\text{BF}_4]$  at room temperature at a scan rate of  $0.2 \text{ V s}^{-1}$  or at other mentioned scan rates.

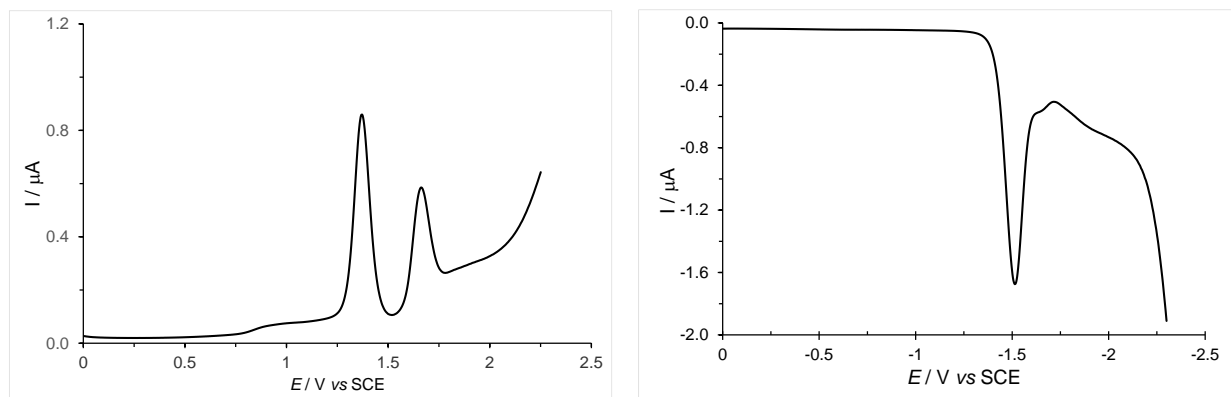


**Figure S12.** OSWVs: anodic (left) and cathodic (right) scans of complex **Re-BPTA**.

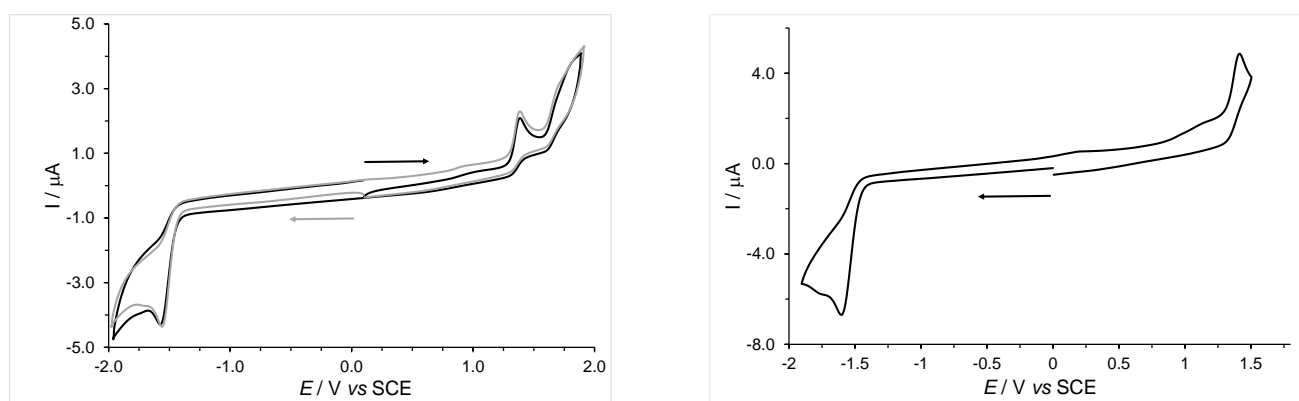


**Figure S13.** Cyclic voltammograms of complex **Re-BPTA** (left) at  $0.2 \text{ V/s}$ , and segmented voltammogram at  $1 \text{ V/s}$  (right).

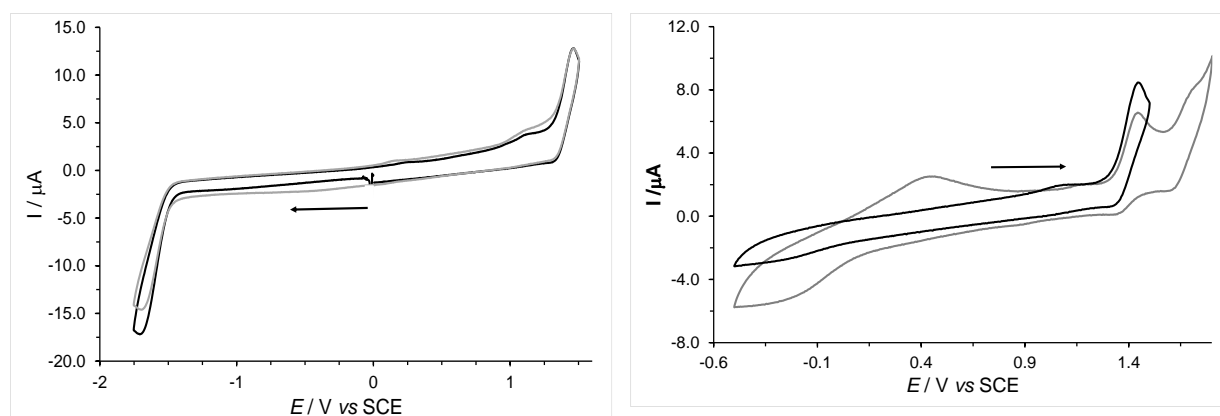


**Figure S14.** Segmented cyclic voltammograms of complex **Re-BPTA** with its first oxidation process and part of its reduction process at  $10 \text{ V/s}$  (left). Segmented cyclic voltammograms of complex **Re-BPTA** at increasing potential, scan 1 (black), scan 2 (grey) at  $10 \text{ V/s}$  (right).

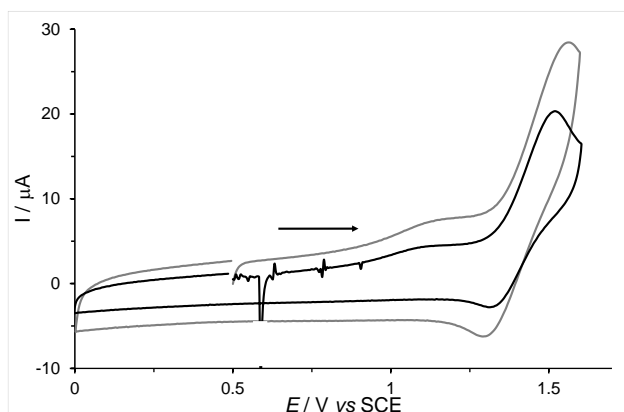


**Figure S15.** Segmented cyclic voltammograms of complex **Re-BPTA**: first oxidation wave at 50 V/s (black) and 100 V/s (grey).

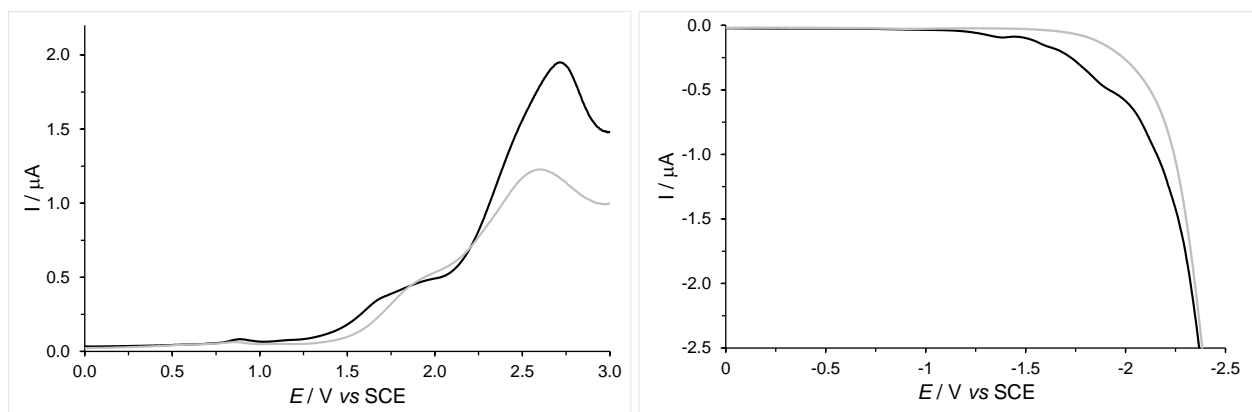


**Figure S16.** OSWVs: anodic (left) and cathodic (right) scans of ligand **BPTA** in black, electrochemical solution without ligand **BPTA** (light grey).

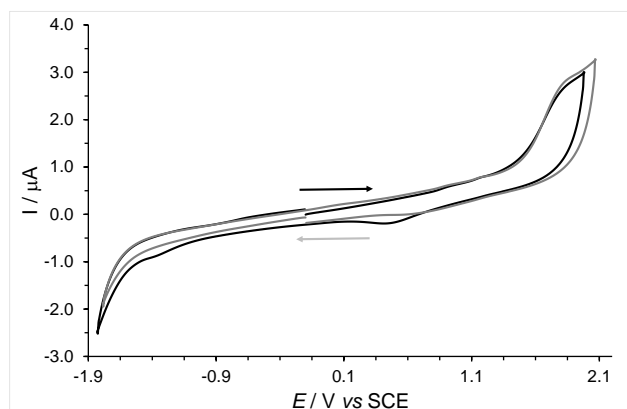


**Figure S17.** Cyclic voltammograms of ligand **BPTA** at 0.2 V/s.

## Spectroscopy

**Table S8.** Solid state spectroscopic data of two samples of **Re-BPTA** obtained from evaporation of butan-2-ol and chloroform. Photoluminescence maximum wavelength ( $\lambda_{\text{PL}}$ ) and quantum yield ( $\Phi_{\text{PL}}$ ) for the pristine powders, ground powders and ground powder fumed with THF for 48 h.

Solvent of preparation	Pristine		Ground		THF fumed	
	$\lambda_{\text{PL}}$	$\Phi_{\text{PL}}$	$\lambda_{\text{PL}}$	$\Phi_{\text{PL}}$	$\lambda_{\text{PL}}$	$\Phi_{\text{PL}}$
Butan-2-ol	546	0.52	548	0.38	546	0.51
Chloroform	554	0.27	554	0.29	---	---

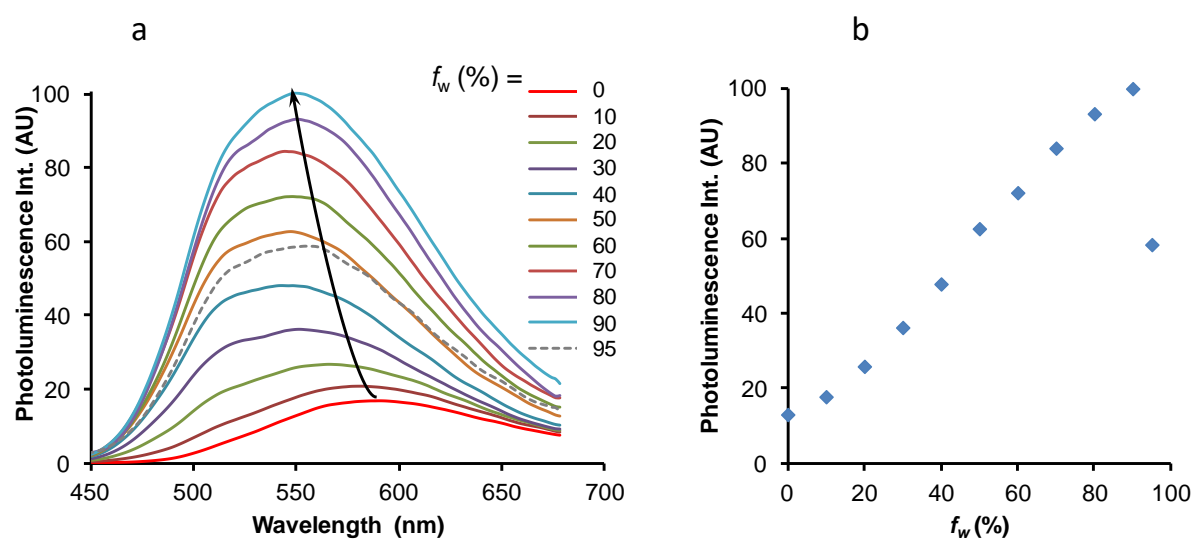


**Figure S18.** a) Emission spectra of complex **Re-BPTA** at  $3.3 \times 10^{-5}$  M in acetonitrile solutions containing from 0 to 95% water,  $\lambda_{\text{ex}} = 350$  nm, recorded 24h after sample preparation. b) Evolution of the PL intensity at 546 nm as a function of the proportion of water in acetonitrile.

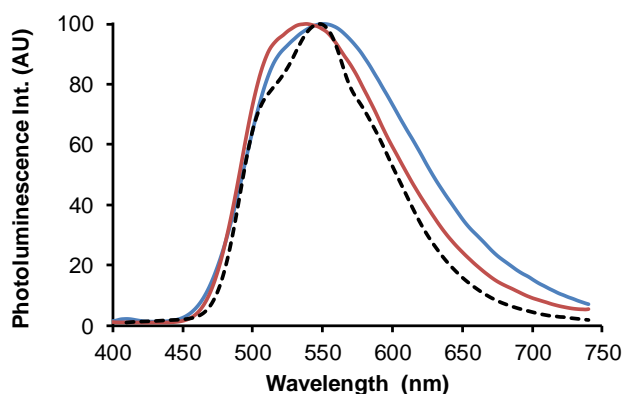


**Figure S19.** Normalized emission spectra of microcrystals of **Re-BPTA** obtained from butan-2-ol as powder (black dotted line) and after dispersion in water (red line), and comparison with the suspension in  $\text{H}_2\text{O}/\text{CH}_3\text{CN}$  90:10 v/v (AIPE experiment, blue line).  $\lambda_{\text{ex}} = 380$  nm. Note that the spectrum of the powder sample was obtained using the integration sphere, and the correction curve is different from that used for the suspensions, which may partly explain some differences in the shape of the spectra.

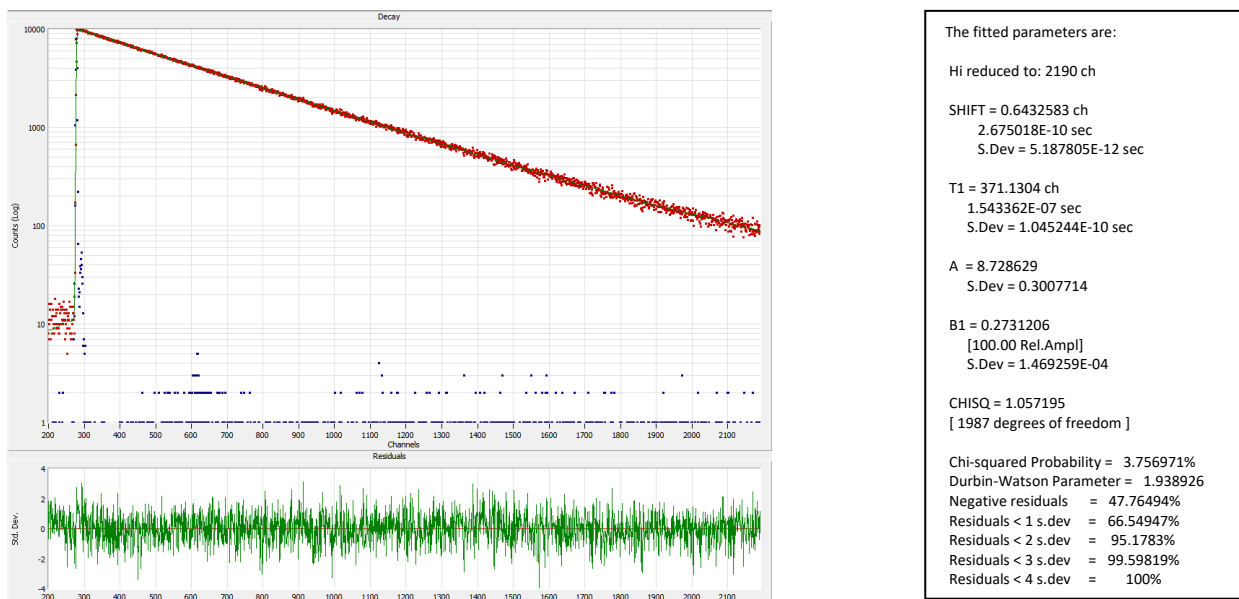


**Figure S20.** Photoluminescence decay of **Re-BPTA** ( $\sim 2.2 \times 10^{-5}$  M) in dichloromethane solution.

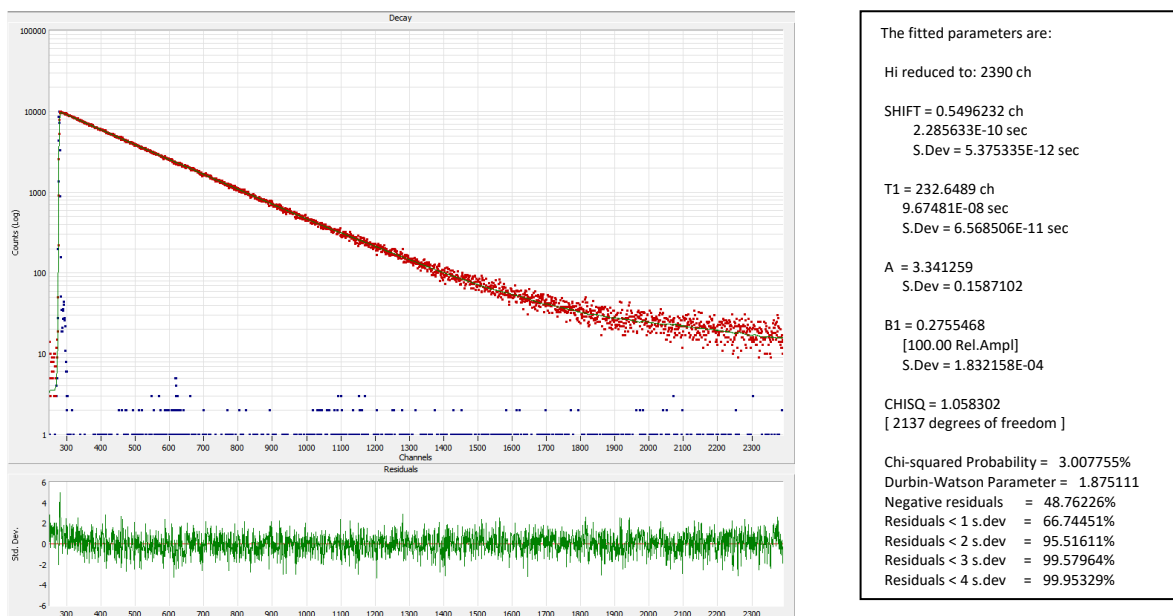
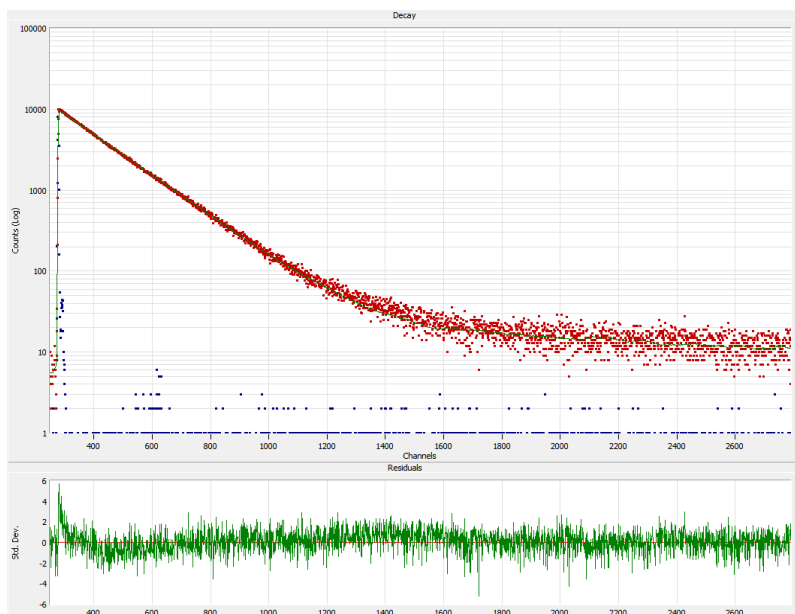


**Figure S21.** Photoluminescence decay of **Re-BPTA** ( $\sim 3.5 \times 10^{-5}$  M) in acetonitrile solution.



The fitted parameters are:

Hi reduced to: 2790 ch

SHIFT = 0.5636638 ch  
 2.344021E-10 sec  
 S.Dev = 5.718794E-12 sec

T1 = 170.8674 ch  
 7.105596E-08 sec  
 S.Dev = 6.407835E-11 sec

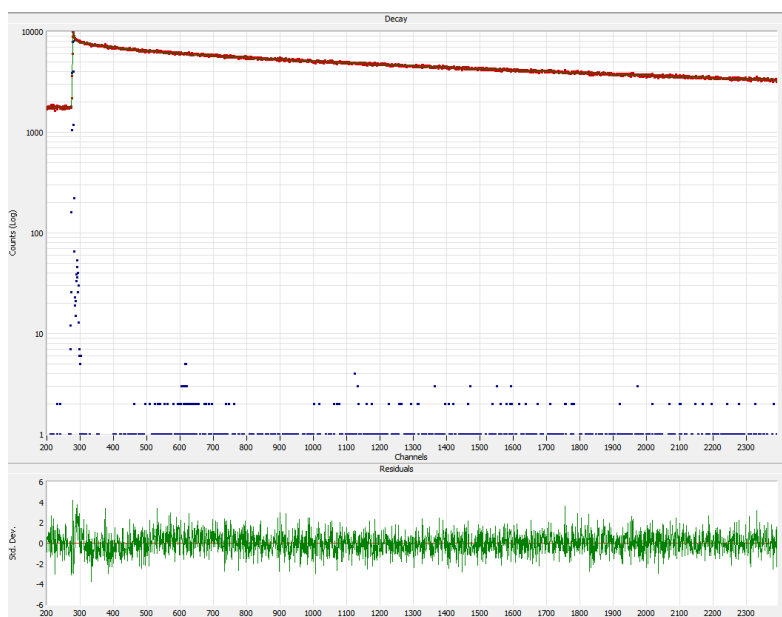
A = 5.521655  
 S.Dev = 9.726106E-02

B1 = 0.2744201  
 [100.00 Rel.Ampl]  
 S.Dev = 2.117749E-04

CHISQ = 1.199984  
 [ 2537 degrees of freedom ]

Chi-squared Probability = 1.0101E-09%  
 Durbin-Watson Parameter = 1.677222  
 Negative residuals = 44.07713%  
 Residuals < 1 s.dev = 64.62023%  
 Residuals < 2 s.dev = 94.13617%  
 Residuals < 3 s.dev = 99.17355%  
 Residuals < 4 s.dev = 99.72452%

**Figure S22.** Photoluminescence decay of **Re-BPTA** ( $\sim 3.0 \times 10^{-5}$  M) in methanol solution.



The fitted parameters are:

Hi reduced to: 2390 ch

SHIFT = -0.1428012 ch  
 -5.938451E-11 sec  
 S.Dev = 8.098814E-12 sec

T1 = 2.560777 ch  
 1.06491E-09 sec  
 S.Dev = 7.529271E-11 sec

T2 = 143.6398 ch  
 5.973323E-08 sec  
 S.Dev = 1.663103E-09 sec

T3 = 1756.192 ch  
 7.303201E-07 sec  
 S.Dev = 2.170165E-09 sec

A = 1760.389  
 S.Dev = 3.621705

B1 = 0.2125034  
 [0.23 Rel.Ampl]  
 S.Dev = 3.73878E-03

B2 = 3.747867E-02  
 [2.23 Rel.Ampl]  
 S.Dev = 3.622585E-04

B3 = 0.1338641  
 [97.54 Rel.Ampl]  
 S.Dev = 1.957775E-04

CHISQ = 1.11256  
 [ 2183 degrees of freedom ]

Chi-squared Probability = 1.6099E-02%  
 Durbin-Watson Parameter = 1.986751  
 Negative residuals = 49.38384%  
 Residuals < 1 s.dev = 66.91009%  
 Residuals < 2 s.dev = 94.43176%  
 Residuals < 3 s.dev = 99.49795%  
 Residuals < 4 s.dev = 99.95436%

**Figure S23.** Photoluminescence decay of **Re-BPTA** microcrystalline powder obtained from butan-2-ol.



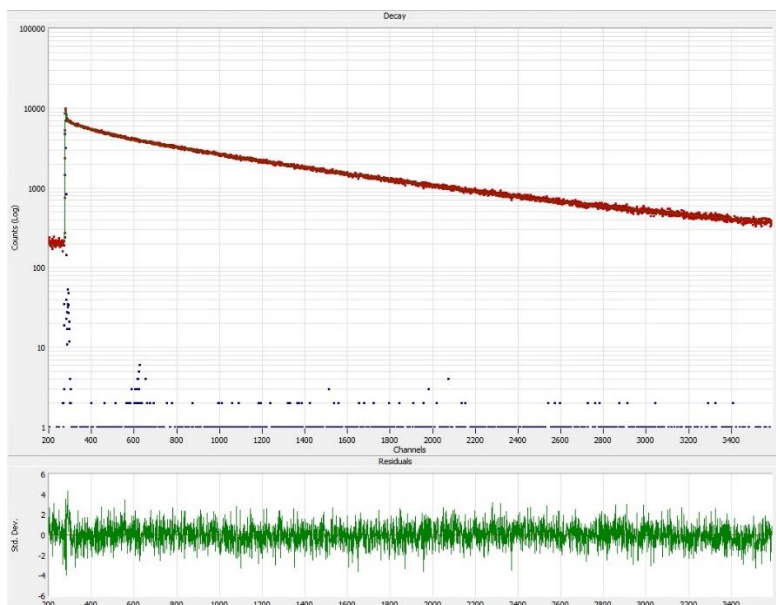


**Figure S24.** Photoluminescence decay of **Re-BPTA** ( $3.3 \times 10^{-5}$  M) in water/acetonitrile 90:10 v/v.

The fitted parameters are:

Hi reduced to: 3590 ch

SHIFT = 0.0547942 ch  
 2.278641E-11 sec  
 S.Dev = 7.305223E-12 sec

T1 = 2.079421 ch  
 8.647364E-10 sec  
 S.Dev = 5.004512E-11 sec

T2 = 139.3021 ch  
 5.792939E-08 sec  
 S.Dev = 1.069665E-09 sec

T3 = 948.6752 ch  
 3.945108E-07 sec  
 S.Dev = 6.438184E-10 sec

A = 197.6246  
 S.Dev = 0.6875767

B1 = 0.3231632  
 [0.48 Rel.Ampl]  
 S.Dev = 4.273481E-03

B2 = 4.701056E-02  
 [4.67 Rel.Ampl]  
 S.Dev = 3.286287E-04

B3 = 0.1401092  
 [94.85 Rel.Ampl]  
 S.Dev = 1.11114E-04

CHISQ = 1.090398  
 [ 3383 degrees of freedom ]

Chi-squared Probability = 0.0147901%  
 Durbin-Watson Parameter = 1.906441  
 Negative residuals = 49.36597%  
 Residuals < 1 s.dev = 66.76497%  
 Residuals < 2 s.dev = 94.60336%  
 Residuals < 3 s.dev = 99.4102%  
 Residuals < 4 s.dev = 99.97051%

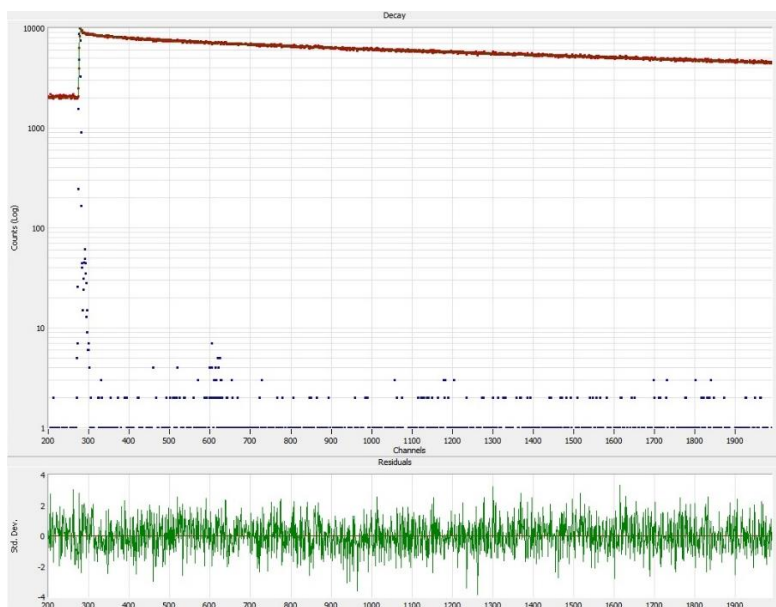


**Figure S25.** Photoluminescence decay of **Re-BPTA** as microcrystalline powder (obtained from butan-2-ol) dispersed in water.

The fitted parameters are:

Hi reduced to: 1990 ch

SHIFT = -5.361325E-02 ch  
 -2.229531E-11 sec  
 S.Dev = 9.830785E-12 sec

T1 = 117.5161 ch  
 4.88696E-08 sec  
 S.Dev = 1.984057E-09 sec

T2 = 2.38046 ch  
 9.899247E-10 sec  
 S.Dev = 7.720603E-11 sec

T3 = 1921.487 ch  
 7.99059E-07 sec  
 S.Dev = 2.375049E-09 sec

A = 2043.585  
 S.Dev = 4.540502

B1 = 2.587917E-02  
 [1.00 Rel.Ampl]  
 S.Dev = 3.99588E-04

B2 = 0.1388587  
 [0.11 Rel.Ampl]  
 S.Dev = 3.916305E-03

B3 = 0.1565757  
 [98.89 Rel.Ampl]  
 S.Dev = 2.085021E-04

CHISQ = 1.051307  
 [ 1783 degrees of freedom ]

Chi-squared Probability = 6.460797%  
 Durbin-Watson Parameter = 2.002228  
 Negative residuals = 49.63707%  
 Residuals < 1 s.dev = 66.7225%  
 Residuals < 2 s.dev = 94.75153%  
 Residuals < 3 s.dev = 99.49749%  
 Residuals < 4 s.dev = 100%

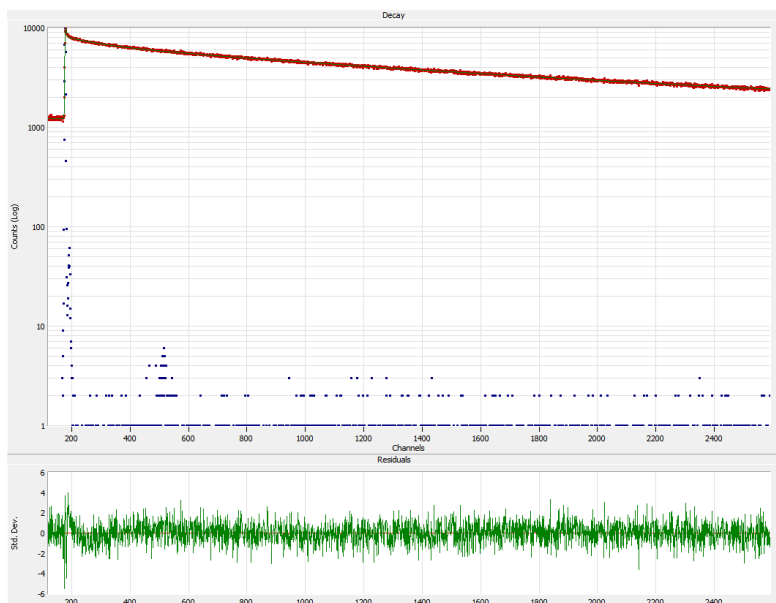


**Figure S26.** Photoluminescence decay of **Re-Phe** microcrystalline powder.

The fitted parameters are:

Hi reduced to: 2590 ch

SHIFT = 0.0514966 ch  
 2.141509E-11 sec  
 S.Dev = 8.355113E-12 sec

T1 = 3.01927 ch  
 1.255577E-09 sec  
 S.Dev = 8.907812E-11 sec

T2 = 143.5256 ch  
 5.968576E-08 sec  
 S.Dev = 1.483393E-09 sec

T3 = 1536.439 ch  
 6.389352E-07 sec  
 S.Dev = 1.592319E-09 sec

A = 1227.893  
 S.Dev = 2.836676

B1 = 0.1616507  
 [0.22 Rel.Ampl]  
 S.Dev = 3.051225E-03

B2 = 3.562143E-02  
 [2.27 Rel.Ampl]  
 S.Dev = 3.515054E-04

B3 = 0.1430173  
 [97.51 Rel.Ampl]  
 S.Dev = 1.725031E-04

CHISQ = 1.073985  
 [ 2463 degrees of freedom ]

Chi-squared Probability = 0.5481262%  
 Durbin-Watson Parameter = 1.88993  
 Negative residuals = 49.73695%  
 Residuals < 1 s.dev = 66.36989%  
 Residuals < 2 s.dev = 94.90085%  
 Residuals < 3 s.dev = 99.55483%  
 Residuals < 4 s.dev = 99.87859%

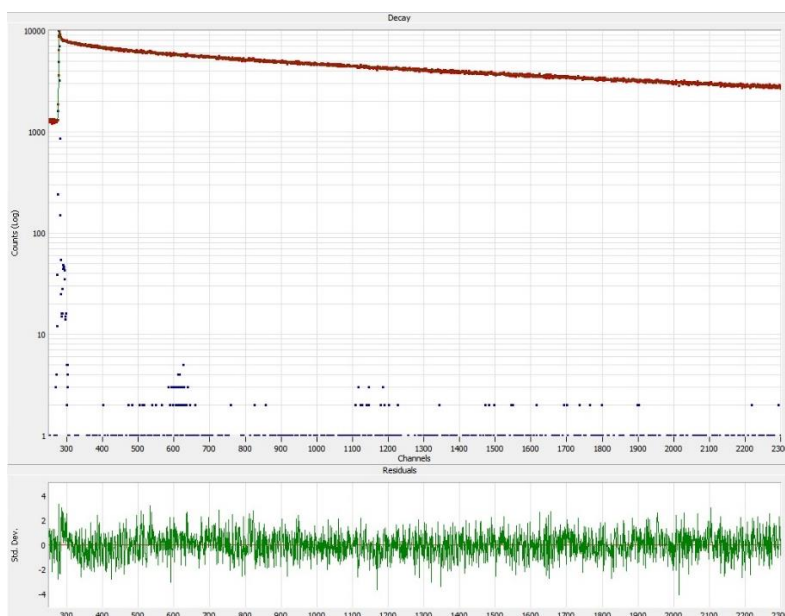


**Figure S27.** Photoluminescence decay of **Re-Phe-Ada** microcrystalline powder.

The fitted parameters are:

Hi reduced to: 2300 ch

SHIFT = -6.739429E-02 ch  
 -2.802622E-11 sec  
 S.Dev = 7.683109E-12 sec

T1 = 2.180721 ch  
 9.068627E-10 sec  
 S.Dev = 5.685307E-11 sec

T2 = 145.4145 ch  
 6.047127E-08 sec  
 S.Dev = 1.644882E-09 sec

T3 = 1553.87 ch  
 6.461837E-07 sec  
 S.Dev = 2.201864E-09 sec

A = 1280.708  
 S.Dev = 4.056493

B1 = 0.2428479  
 [0.23 Rel.Ampl]  
 S.Dev = 4.221174E-03

B2 = 3.713449E-02  
 [2.36 Rel.Ampl]  
 S.Dev = 3.730864E-04

B3 = 0.1435503  
 [97.41 Rel.Ampl]  
 S.Dev = 2.26044E-04

CHISQ = 1.070533  
 [ 2043 degrees of freedom ]

Chi-squared Probability = 1.344119%  
 Durbin-Watson Parameter = 1.891855  
 Negative residuals = 48.7567%  
 Residuals < 1 s.dev = 66.69917%  
 Residuals < 2 s.dev = 94.44173%  
 Residuals < 3 s.dev = 99.60995%  
 Residuals < 4 s.dev = 99.95124%